ON TRANSITION REGIONS FOR THE SIMULATION OF THE MECHANICAL RESPONSE OF COMPOSITE MATERIALS AT MULTIPLE LENGTH-SCALES

L. Gigliotti*[1], S. T. Pinho[1]

[1] *Department of Aeronautics, Imperial College London, London SW7 2AZ, United Kingdom*
* *Corresponding Author: l.gigliotti12@imperial.ac.uk*

Keywords: Multiscale modelling, Mesh Superposition Technique, Composite materials, Damage simulation

Abstract

A novel Mesh Superposition Technique (MST) for the transition between differently-discretized subdomains is proposed and implemented in a FE code. The interfaces between these subdomains are replaced by transition regions where the corresponding meshes are superposed. As a result, the artificial stress wave reflections and stress concentrations at these interfaces are eliminated. The MST is applied to the low-velocity impact of a projectile on a composite plate. The use of the MST allows to retrieve the same results of a fully refined model, unlike a multiscale approach with a sudden discretization-transition. Compared to the latter, the MST uses similar computational times. Furthermore, the MST is successfully utilized for a 3D-2D coupling, achieving a 73% computational time reduction with respect to the fully 3D model, even for a small component.

1. Introduction

Numerical simulation of the mechanical response of large composite structures often requires different parts to be modelled at different scales, eventually even using different physics. Furthermore, since multiscale modelling techniques allow the development of numerical models with a non-uniform level of refinement across the investigated domain, they can achieve the required level of accuracy in each part of the model while minimizing the computational time.

However, in dynamic problems involving fracture and progressive failure, abrupt changes in both finite element type and size lead to artificial stress wave reflections and unrealistic stress concentrations at the interfaces between differently-discretized subdomains. As a result, the mechanical response of the composite structure is not correctly replicated and the prediction of damage initiation and evolution is not accurate.

The problem of spurious stress wave reflections[1] at the interface between differently-discretized

[1] These reflected waves are referred to as spurious since they do not exist in reality, i.e. are not reflected when propagating through homogeneous elastic media, but are related to the change in the finite element grid. Spurious wave reflection at these interfaces occurs as if they represented the interface between two different continuous media.

domains was firstly addressed by Kuhlmeyer and Lysmer [1] and by Bažant [2]. Several approaches, including the use of transition regions where the elements' size is progressively reduced [3] and of higher-order elements [4], have been suggested to mitigate such drawback.

Bridging methods for coupling continuum models with atomistic models, as well as discrete and finite element models, have been proposed by Belytschko and Xiao [5, 6], Rojek and Oñate [7] and Lee and Basaran [8]. In the approach described in [5, 6], bridged subdomains overlap at the shared interface as in the method proposed here.

In this work, we present a novel numerical technique for a gradual element-type transition between differently-discretized subdomains. The interfaces between domains whose FE discretizations consist of different element types are replaced by regions where the corresponding discretizations are superposed. The energy equivalence is satisfied by scaling the stiffness and mass matrices associated with each pair of elements sharing the same set of nodes. This scaling is achieved by means of positive piecewise-continuous weighting functions over the transition subdomains.

The MST is applied to the low-velocity impact of a projectile on a composite plate, showing to correctly predict the damage pattern, unlike a multiscale approach with a sudden discretization-transition. Compared to the latter, the MST uses similar computational times. Furthermore, the MST is used to couple three-dimensional refined discretizations to two-dimensional discretizations. The effectiveness of this approach is demonstrated by the approximately 73% computational time reduction obtained, with respect to the fully three-dimensional model, even for a small component.

2. Mesh Superposition Technique

2.1. Theory

Let us consider a deformable body $\mathcal{B}$ occupying the domain $\omega(t) \in \mathbb{R}^3$, where with $\mathbb{R}^3$ we denote the three-dimensional euclidean space, for any instant of time $t > 0$. In addition, we indicate the domain occupied by the deformable body at the instant $t = 0$ with Ω. The position of each generic point $P \in \Omega$ can be expressed with respect to an arbitrary origin O by the position vector $\mathbf{X}$.

Further, we consider the domain Ω to be subdivided into the subdomains Ω_A and Ω_B, whose intersection is not the empty set, i.e. the two subdomains overlap over the subdomain $\Omega_\mathrm{s} = \Omega_\mathrm{A} \cap \Omega_\mathrm{B}$. Additionally, it is convenient to decompose the subdomains Ω_A and Ω_B as shown in Figure 1, i.e. into an overlapping portion Ω_s and a non-overlapping one defined as

$$\widehat{\Omega}_i = \Omega_i \setminus \Omega_\mathrm{s} \qquad \text{for} \quad i = \mathrm{A}, \mathrm{B}. \tag{1}$$

Within the subdomain Ω_s, where univocal definitions of the second Piola-Kirchhoff stress tensor $\mathbf{S}$ and of the material density ρ do not exist, these can be expressed as the linear combination of the contributions relative to the superposed subdomains.

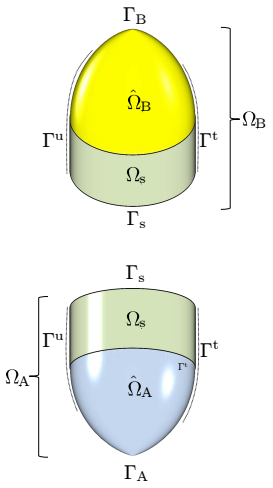

Figure 1. The domain Ω can be decomposed into the subdomains Ω_A and Ω_B which overlap over the subdomain Ω_s.

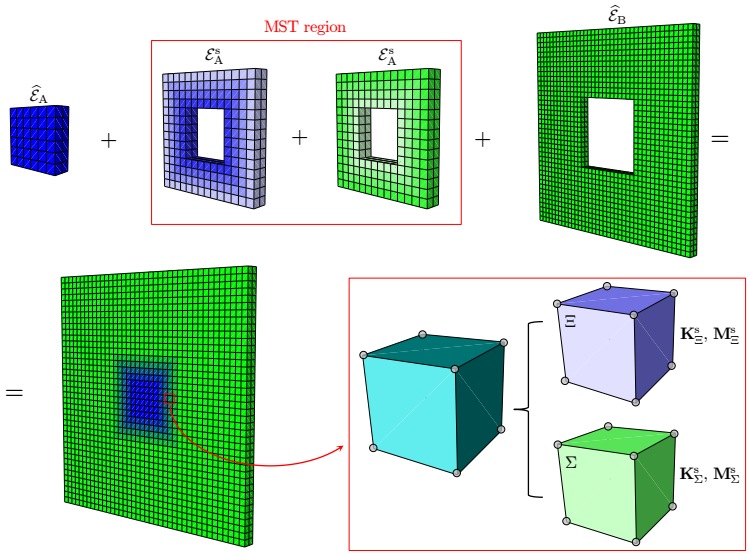

Figure 2. FE meshes of the superposed subdomains Ω_A and Ω_B. Within the overlapping region, the two meshes are superposed, and the nodal connectivity coincidence enforced. For each element $\Xi \in \mathcal{E}_A$, there is a second element $\Sigma \in \mathcal{E}_B$ such that these two elements share the nodes and the centroid's position.

These contributions are scaled by non-negative scalar-valued weighting factors $\psi_i(\mathbf{X})$, continuous over the subdomain Ω_s. These coefficients are computed as function of the position vector $\mathbf{X}$ in the reference configuration and, as such, do not vary as the body deforms. This leads to a significant advantage in terms of both FE implementation and computational cost since no remeshing is needed. Hence, an equivalent second Piola-Kirchhoff stress tensor $\mathbf{S}_s$ and material mass density ρ_s can be defined as

$$\mathbf{S}_s(\mathbf{X},t) = \sum_{i\in\{A,B\}} \psi_i(\mathbf{X})\mathbf{S}_i(\mathbf{X},t) \quad \text{and} \quad \rho_s(\mathbf{X}) = \sum_{i\in\{A,B\}} \psi_i(\mathbf{X})\rho_i(\mathbf{X}). \tag{2}$$

For the sake of completeness, it may be demonstrated that, in order to satisfy the conservation of mass principle, the collection of weighting factors $\psi_i(\mathbf{X})$ represents a partition of unity of the subdomain $\Omega_s = \text{supp}\,(\psi_i(\mathbf{X}))$, i.e.

$$\sum_{i\in\{A,B\}} \psi_i(\mathbf{X}) = 1 \qquad \forall P(\mathbf{X}) \in \Omega_s. \tag{3}$$

2.2. Finite Element implementation

The FE implementation of the MST can be visualized in Figure 2. The scaling of the second Piola-Kirchhoff stress tensor, prescribed in Equation 2, is numerically obtained by scaling the stiffness matrices of elements Ξ and Σ within the transition region, through the piece-wise continuous weighting factors $\psi_\Xi(\mathbf{X}_C)$ and $\psi_\Sigma(\mathbf{X}_C)$, i.e.

$$\mathbf{K}_{\mathrm{s}}^{\Xi} = \int_{\Xi} \mathbf{B}_{\Xi}^{\mathrm{T}} \,:\, \psi_{\Xi}(\mathbf{X}_C)\Big(\mathbf{I} \otimes \mathbf{S}_{\mathrm{A}} + \mathbf{F}\mathbb{C}_{\mathrm{A}}\mathbf{F}^{\mathrm{T}}\Big) \,:\, \mathbf{B}_{\Xi}\, \mathrm{d}\Xi \quad \text{and}$$

$$\mathbf{K}_{\mathrm{s}}^{\Sigma} = \int_{\Sigma} \mathbf{B}_{\Sigma}^{\mathrm{T}} \,:\, \psi_{\Sigma}(\mathbf{X}_C)\Big(\mathbf{I} \otimes \mathbf{S}_{\mathrm{B}} + \mathbf{F}\mathbb{C}_{\mathrm{B}}\mathbf{F}^{\mathrm{T}}\Big) \,:\, \mathbf{B}_{\Sigma}\, \mathrm{d}\Sigma. \tag{4}$$

where $\mathbf{B}_{\Xi}$ and $\mathbf{B}_{\Sigma}$ are the element shape functions derivatives matrices of finite elements Ξ and Σ, respectively and $\mathbf{X}_C$ denotes the element's centroid position. Since ψ_{Ξ} and ψ_{Σ} are computed as function of the elements' centroid coordinates in the undeformed configuration, their values do not change as the body deforms, therefore, no re-meshing is required during the analysis.

Similarly, the mass matrices of elements Ξ and Σ within the transition region, may be computed following a similar approach to the one used for the stiffness matrices in Equation 4, i.e.

$$\mathbf{M}_{\mathrm{s}}^{\Xi} = \int_{\Xi} \psi_{\Xi}(\mathbf{X}_C)\, \rho_{\mathrm{A}} \mathbf{N}_{\Xi}^{\mathrm{T}} \mathbf{N}_{\Xi}\, \mathrm{d}\Xi \quad \text{and}$$

$$\mathbf{M}_{\mathrm{s}}^{\Sigma} = \int_{\Sigma} \psi_{\Sigma}(\mathbf{X}_C)\, \rho_{\mathrm{B}} \mathbf{N}_{\Sigma}^{\mathrm{T}} \mathbf{N}_{\Sigma}\, \mathrm{d}\Sigma. \tag{5}$$

3. Applications

3.1. Low-velocity impact on a composite plate - 3D-to-3D coupling

In the present work, the MST detailed previously is used to simulate the low-velocity impact response of $[0_3^\circ/90_3^\circ]_{\mathrm{s}}$ cross-ply laminates made of HS160/REM graphite/epoxy, investigated experimentally and numerically by Aymerich et al. [9]. The specimens were rectangular with 65.0 mm×87.5 mm in-plane dimensions and a 2.0 mm average thickness. The specimens were impacted with a 2.3 kg hemispherical nose steel tup of 12.5 mm of diameter and were simply supported on a steel plate with a rectangular (45.0 mm×67.5 mm) opening.

The impact-induced damage consists of an initial tensile matrix crack in the distal 0° layers, followed by a two-lobe shaped delamination at the bottom 0°/90° interface. For impact energy higher than 5 J, localized matrix crushing is observed at the impact location and, for impact energy of approximately 7 J, delaminations develop at the top 0°/90° interface.

Three different FE models of the specimen were built: (i) a fully refined model (FR) shown in Figure 3(a), (ii) a model with a sudden-discretization transition (ST) shown in Figure 3(b) and (iii) a model where the sudden discretization-transition is replaced by transition regions where the meshes are superposed (MST) as shown in Figure 3(c). Because of the symmetry, only one quarter of the specimen was modelled. The simply supported boundary conditions were enforced by constraining the vertical displacement of the nodes initially lying on the edges of

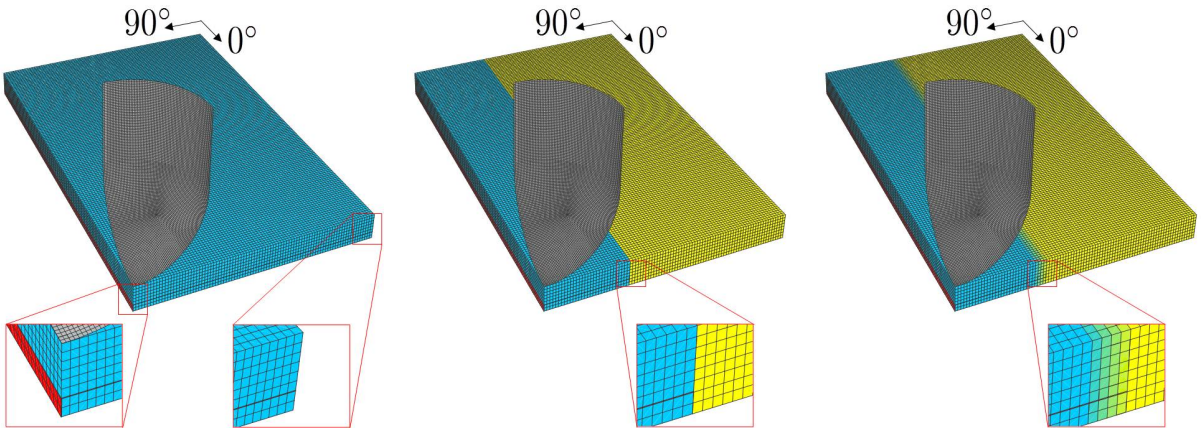

(a) FR model. (b) ST model. (c) MST model.

Figure 3. The low-velocity impact was simulated using three different FE models. In the fully refined (FR) model, the plies were discretized with 3D eight-noded solid elements (light blue) while for the ST and MST models, solid elements were used only within the area surrounding the impact location. In the remaining structure, eight-noded continuum shell elements (yellow) were used. Interlaminar damage and tensile matrix cracking were simulated using cohesive elements (red). The MST transition region is represented with layers of different green tonalities.

the opening support. For the FR model, each of the 0°_3 and 90°_3 sublaminates were modelled with two 3D eight-noded brick elements through their thickness. Since an impact energy of 3.1 J was considered, the onset and growth of interlaminar damage was modelled by inserting a layer of cohesive elements at the bottom $0^\circ/90^\circ$ interface. Analogously, the intralaminar matrix tensile cracking was simulated using cohesive elements placed at the symmetry plane parallel to the 0°-plies direction.

In the ST and MST models the plies were modelled using 3D eight-noded brick elements only in the area surrounding the impact location; for the remaining part eight-noded continuum shell elements were used. These discretizations were superposed over a region of four elements in the laminate plane and cohesive elements were used between plies only when these were modelled with 3D solid elements. Elastic material properties used for the simulations are summarized in Table 1.

Table 1. Elastic properties of the plies and cohesive properties of the interfaces used for the simulations.

E_{11}		$E_{22} = E_{33}$		$G_{12} = G_{13} = G_{23}$	$\nu_{12} = \nu_{13} = \nu_{23}$
93.7 GPa		7.45 GPa		3.97 GPa	0.261
k_N	$k_S = k_T$	N	$S = T$	G_{Ic}	$G_{\mathrm{IIc}} = G_{\mathrm{IIIc}}$
120 GPa/mm	43 GPa/mm	30 MPa	80 MPa	520 J/m^2	970 J/m^2

The interlaminar damage pattern at the bottom $0^\circ/90^\circ$ interface, simulated with the three FE models considered in this example, is shown in Figure 4.

The MST model retrieves the same results of the FR model, unlike a multiscale approach with a sudden discretization-transition (ST model). The latter is shown not to capture the correct delamination pattern, predicting the failure of the cohesive elements at the interface between the differently-discretized subdomains, regardless of the position of this interface. This drawback is completely eliminated by the MST proposed in this paper. However, this is achieved at a small computational cost as shown in Figure 5.

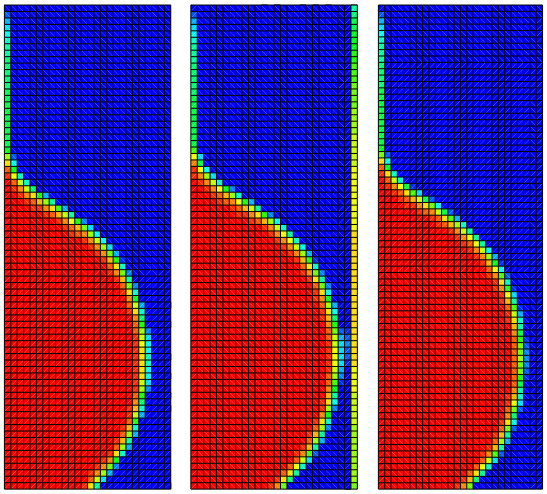

(a) FR model. (b) ST model. (c) MST model.

Figure 4. Predicted interlaminar damage pattern at the bottom 0°/90° interface. Completely failed elements are shown in red while blue is associated to undamaged elements.

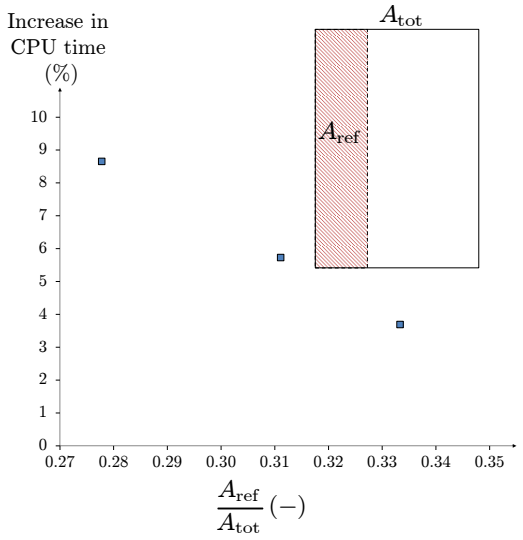

Figure 5. Increment in the computational time for the MST model with respect to the ST model. The additional computational time decreases as the ratio between the refined in-plane area A_{ref} and the total in-plane area A_{tot} increases.

3.2. Low-velocity impact on a composite plate - 3D-to-2D coupling

In this second example, the MST is used to couple a three-dimensional discretization to a two-dimensional discretization. Similarly to the first example, we considered the low-velocity impact on simply supported $[0_2^\circ/90_2^\circ/0_2^\circ]_s$ cross-ply laminates made of HS160/REM graphite/epoxy.

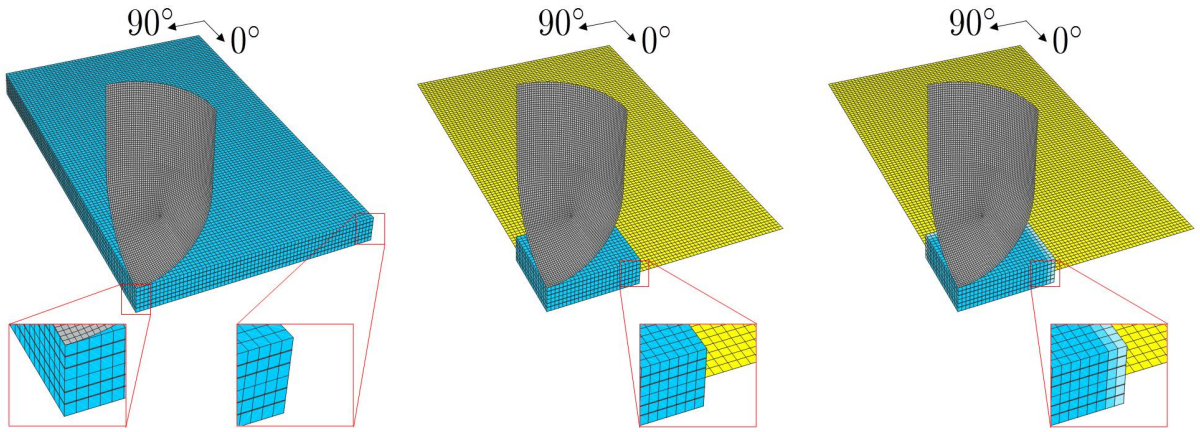

(a) FR model. (b) ST model. (c) MST model.

Figure 6. The low-velocity impact was simulated using three different FE models. In the fully refined (FR) model, the plies were discretized with 3D eight-noded solid elements (light blue) while for the ST and MST models, these elements were used only within the area surrounding the impact location. In the remaining structure, four-noded composite shell elements (yellow) were used. Delamination was simulated using cohesive elements in the 3D region.

Three different FE models of the specimen were built: (i) a fully refined model (FR) shown in

Figure 6(a), (ii) a model with a sudden discretization-transition (ST) shown in Figure 6(b) and (iii) a model where the sudden discretization-transition is replaced by transition regions where the meshes are superposed (MST) as shown in Figure 6(c). Because of the symmetry, only one quarter of the specimen was modelled.

For the FR model, each of the 0°_{2} and 90°_{2} sublaminates was modelled with a single 3D eight-noded brick element through their thickness. The onset and growth of interlaminar damage was modelled by inserting layers of cohesive elements at the interfaces between differently oriented plies. Unlike the previous example, the matrix tensile cracking was not simulated. In the ST and MST models, the plies are modelled using 3D eight-noded brick elements only in the area surrounding the impact location; for the remaining of the structure, four-noded composite shell elements were used.

The discretizations were superposed over a transition region of two elements in the laminate plane and cohesive elements were used between plies only when these were modelled with 3D solid elements. Elastic material properties used for the simulations are summarized in Table 1.

The interlaminar damage pattern at the interface between differently oriented plies, simulated with the three FE models considered in this example, is shown in Figures 7 - 9. Delamination does not occur at the distal 0°/90° interface.

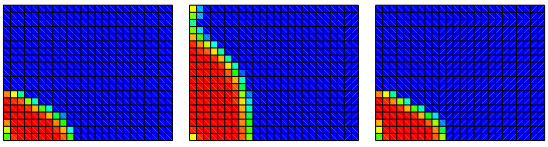

(a) FR model. (b) ST model. (c) MST model.

Figure 7. Predicted interlaminar damage pattern at the 1st 0°/90° interface.

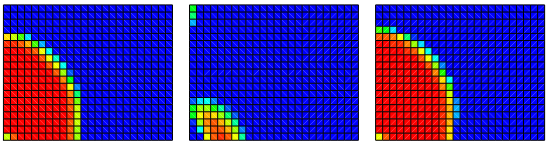

(a) FR model. (b) ST model. (c) MST model.

Figure 8. Predicted interlaminar damage pattern at the 2nd 0°/90° interface.

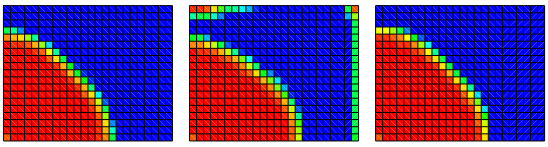

(a) FR model. (b) ST model. (c) MST model.

Figure 9. Predicted interlaminar damage pattern at the 3rd 0°/90° interface.

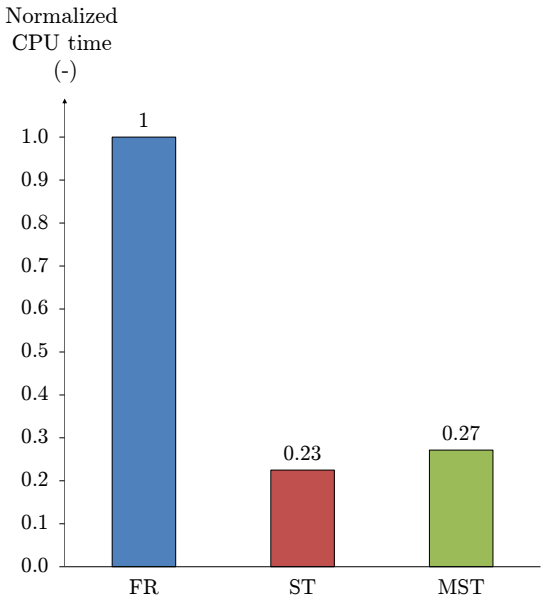

Figure 10. Normalized computational time of the simulations using the FR model, the ST model and the MST model. Unlike the ST model, the MST is capable of significantly reducing the computational effort required (≈ 73% reduction) while predicting the damage pattern correctly.

The results show that, on the one hand the ST model completely fails to predict the delamination

pattern; on the other hand, using the MST it is possible to achieve the same results obtained with a fully three-dimensional model, at an approximate 73% computational time reduction (see Figure 10).

4. Conclusions

A novel Mesh Superposition Technique (MST) for the mesh-transition between differently-discretized subdomains has been presented in this paper. The interfaces between domains whose FE discretizations consist of different element types are replaced by regions where the corresponding discretizations are superposed. In order to satisfy the energy equivalence, the stiffness and mass matrices associated with each pair of elements sharing the same set of nodes are scaled using positive piecewise-continuous weighting functions over the transition subdomains. The advantages of the proposed MST have been demonstrated for the case of low-velocity impact on composite plates. For the case of 3D-to-3D coupling, the MST has been shown to correctly predict the damage pattern, as opposed to a multi-scale approach with a sudden discretization-transition, and at a comparable computational time. Furthermore, the MST is applied to the 3D-to-2D coupling; the results demonstrate that, while a sudden discretization-transition approach does not accurately replicate the damage pattern, the MST retrieves the same results of a fully three-dimensional mesh at only 27% of the computational time.

References

[1] R.L. Kuhlemeyer and J. Lysmer. Finite element method accuracy for wave propagation problems. *Journal of Soil Mechanics & Foundations Div*, 99(Tech Rpt), 1973.

[2] Z. Bažant. Spurious reflection of elastic waves in nonuniform finite element grids. *Computer Methods in Applied Mechanics and Engineering*, 16(1):91–100, 1978.

[3] Z. Celep and Z.P. Bažant. Spurious reflection of elastic waves due to gradually changing finite element size. *International Journal for Numerical Methods in Engineering*, 19(5):631–646, 1983.

[4] Z.P. Bažant and Z. Celep. Spurious reflection of elastic waves in nonuniform meshes of constant and linear strain unite elements. *Computers & Structures*, 15(4):451–459, 1982.

[5] T. Belytschko and S-P. Xiao. Coupling methods for continuum model with molecular model. *International Journal for Multiscale Computational Engineering*, 1(1), 2003.

[6] S-P. Xiao and T. Belytschko. A bridging domain method for coupling continua with molecular dynamics. *Computer methods in applied mechanics and engineering*, 193(17):1645–1669, 2004.

[7] J. Rojek and E. Oñate. Multiscale analysis using a coupled discrete/finite element model. *Interaction and Multiscale Mechanics*, 1(1):1 – 31, 2007.

[8] Y. Lee and C. Basaran. A multiscale modeling technique for bridging molecular dynamics with finite element method. *Journal of Computational Physics*, 253:64 – 85, 2013.

[9] F. Aymerich, F. Dore, and P. Priolo. Prediction of impact-induced delamination in cross-ply composite laminates using cohesive interface elements. *Composites science and technology*, 68(12):2383–2390, 2008.